

The p – T – x -State Diagram of the Mg–Ni System

Yu.V. Levinsky^{1*}, M.M. Alymov^{1,2}, L.L. Rokhlin²

¹ Merzhanov Institute of Structural Microkinetics and Materials Science of RAS,
8, Academician Osipyan Str., Chernogolovka, 432142, Russia;

² Institute of Russian Academy of Sciences A.A. Baykov Metallurgy and Materials Science RAS,
49, Leninsky Prospect, Moscow, 119334, Russia

* Corresponding author: Tel.: +7 496 524 63 84. E-mail: levinsky35@mail.ru

Abstract

The analysis of equilibrium in the Mg–Ni system was carried out. Alloys on its basis are promising for use as sorbents and hydrogen storage (START). The conditions for the production and operation of such alloys imply strict control of the pressure of hydrogen. In this regard, phase equilibria in the Mg–Ni system must be considered not only depending on the composition and temperature, but also on the pressure of hydrogen.

The most complete graphical representation of the equilibrium in the Mg–Ni system is given by a three-dimensional state diagram: pressure-temperature-composition (p – T – x), the projection of the three-phase equilibrium lines of this diagram on the pressure-temperature plane (p – T -state diagram), isobaric and isothermal sections of the diagram, diagram in p_{Mg} – T coordinates.

Based on the analysis of experimental data on equilibrium in this system, the article presents the most important options of the listed types of diagrams.

The presented diagram variants can be useful in optimizing the technology and operation of sorbents and START alloys of the Mg–Ni system.

Keywords

Phase equilibria; structural diagrams; magnesium–nickel alloys; hydrogen storage.

© Yu.V. Levinsky, M.M. Alymov, L.L. Rokhlin, 2020

Introduction

Alloys of the Mg–Ni system are of interest as hydrogen sorbents and alloys of hydrogen storage rings (START) [1–17]. They have a relatively high hydrogen capacity, are convenient in terms of temperature and hydrogen pressure, and sorption and desorption parameters. In addition, some of these alloys have prospects for use as structural materials [11, 13]. In this regard, the study of phase equilibria in the Mg–Ni system with the participation of the gas phase is of interest from the point of view of improving the production technology of magnesium-thermal nickel alloys and magnesium nickelides [18].

Construction a p – T – x -state diagram

The mutual solubility in the solid state in the nickel-magnesium system is very small. The solubility of nickel in magnesium even at 500 °C is less than 0.04 %, the solubility of magnesium in nickel

at 1100 °C is less than 0.2 % (at.). Two intermetallic compounds are formed in the system: Mg₂Ni (hP18) and MgNi₂ (hP24, MgNi₂).

The projection of the lines of maximum solubility of the magnesium-nickel system located in the three-coordinate p – T – x space on the temperature-composition plane is shown in Fig. 1 [19, 20].

The equilibrium gas over Ni–Mg alloys consists mainly of magnesium vapor. The partial vapor pressure of magnesium can be taken as the total vapor pressure even over biphasic MgNi₂ + Ni alloys.

The equilibrium pressure of magnesium vapor for a wide range of concentration and temperature is presented in Table 1 [21–23]. The data of [21, 23] are in good agreement with each other, and they will be taken into account in future calculations.

In the p – T diagram of the Ni–Mg system (Fig. 2), which is the projection of the lines of three-phase equilibria located in three-dimensional p – T – x space

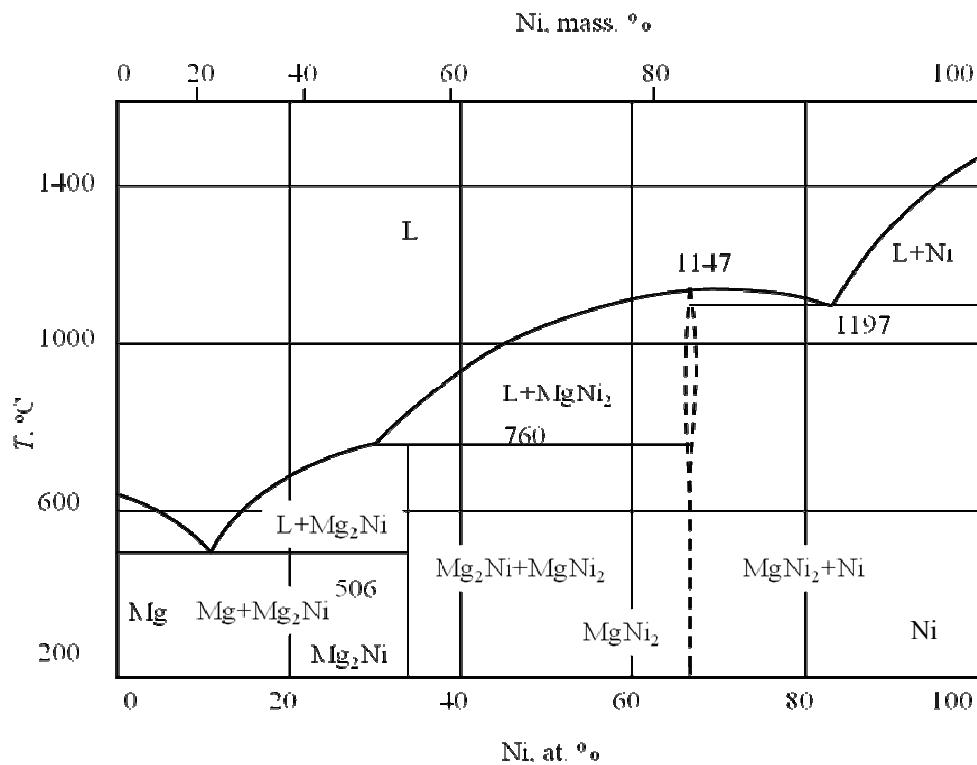


Fig. 1. The projection of the lines of maximum solubility in the nickel – magnesium system on the temperature – composition plane [19, 20]

Table 1

The temperature dependence constants ($\log P_{\text{Mg}} \text{ (Pa)} = A/T + B$) of the partial pressure of Mg vapor over Ni–Mg alloys

Equilibrium phases	Content Ni, at. %	A	B	Temperature range	Source
Mg ₂ Ni+MgNi ₂	33 – 66	8840	11.545	400 – 600	[21]
MgNi ₂ + Ni	>66.7	10700	11.254	560 – 800	[21]
Melt	4.9	6580	9.673	583 – 691	[22]
Melt	11.3	6610	9.700	597 – 700	[22]
Melt +Mg ₂ Ni	19.6	63.50	9.370	597 – 706	[22]
Mg ₂ Ni + MgNi ₂	33.6	7810	10.664	683 – 734	[22]
MgNi ₂ + Ni	> 66	11120	111.945	870 – 932	[22]
Melt	4.2	6730	9.81	650 – 730	[23]
Melt	17.4	6752	9.80	650 – 730	[23]
Mg ₂ Ni + MgNi ₂	47.3	7850	10.65	650 – 730	[23]
Mg ₂ Ni + Ni	70.5	10720	11.86	850 – 930	[23]

onto the pressure – temperature plane, curves 1 – 6, 6 – 14, and 6 – 12 represent evaporation, boiling, and melting of magnesium.

Lines 5 – 14, 6 – 12, 7 – 13, 8 – 15, and 10 – 16 of the equilibrium of only the condensed phases are almost vertical, since in the range of Fig. 2 the pressure does not significantly affect the equilibrium temperature of the condensed phases [24].

The four-phase equilibrium $\text{Mg} \rightleftharpoons \text{Mg}_2\text{Ni} \rightleftharpoons \text{L} \rightleftharpoons \text{G}$ takes place at point 5 ($T = 506 \text{ }^\circ\text{C}$, $p = 16 \text{ Pa}$) [22]. Four curves of three-phase equilibria come out from this point: 5–6, 5–11, 5–2 and 5–7. Curves 5–6 and 5–2 of the equilibria $\text{Mg} \rightleftharpoons \text{L} \rightleftharpoons \text{G}$ and $\text{Mg} \rightleftharpoons \text{Mg}_2\text{Ni} \rightleftharpoons \text{G}$ almost coincide with curve 1–6 of the evaporation of pure magnesium, whereas curve 5–7 of the equilibrium $\text{Mg}_2\text{Ni} \rightleftharpoons \text{L} \rightleftharpoons \text{G}$ was plotted using experimental data work [22].

Table 2

The coordinates of the four-phase equilibrium points of the nickel-magnesium system

Point number on p - T diagram	Temperature, °C	Pressure, Pa	Phases involved in equilibrium
5	506	16	Mg, Mg ₂ Ni, L, G
7	760	$1,3 \cdot 10^3$	Mg ₂ Ni, MgNi ₂ , L, G
8	1097	$6,5 \cdot 10^3$	MgNi ₂ , Ni, L, G

At point 7 ($T = 760$ °C, $p = 1.3 \cdot 10^3$ Pa), the four-phase equilibrium $Mg_2Ni \rightleftharpoons MgNi_2 \rightleftharpoons L \rightleftharpoons G$ at 600–730 °C is plotted according to the data [22, 23], and the curve 7–10–8 of the equilibrium $MgNi_2 \rightleftharpoons L \rightleftharpoons G$ is plotted approximately.

Point 8 ($T = 1097$ °C, $p = 6.5 \cdot 10^3$ Pa) denotes the four-phase equilibrium $MgNi_2 \rightleftharpoons Ni \rightleftharpoons L \rightleftharpoons G$. Curve 4–8 of the three-phase equilibrium $Mg_2Ni \rightleftharpoons MgNi_2 \rightleftharpoons G$ at temperatures 850–930 °C is plotted according to the data [22, 23]. Equilibrium curve 8–9 Ni $\rightleftharpoons L \rightleftharpoons G$ ends at low pressure at the triple point of pure nickel at a temperature of 1455 °C.

The coordinates of the key points of the four-phase equilibrium of the p - T state diagram of the nickel-magnesium system are summarized in Table 2.

The p - T phase diagram of the nickel-magnesium system shown in Fig. 2 is the basis for constructing isobaric and isothermal sections of this system at various pressure and temperature values.

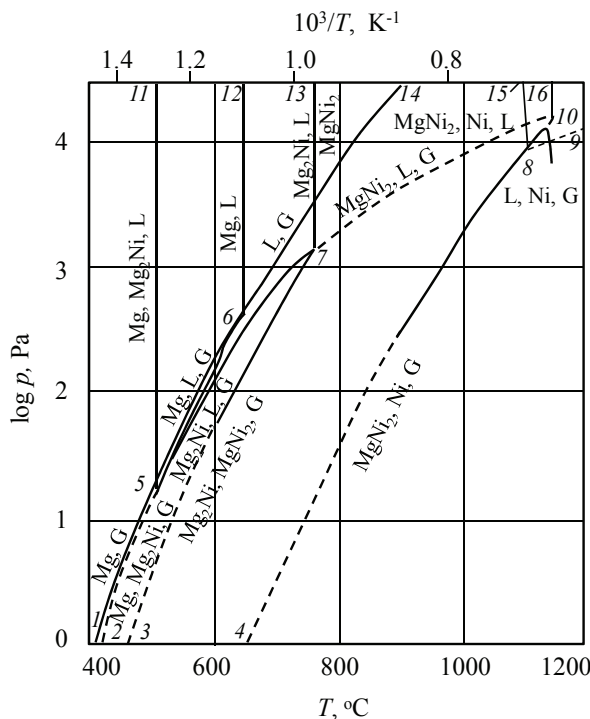


Fig. 2. p - T state diagram of the nickel-magnesium system

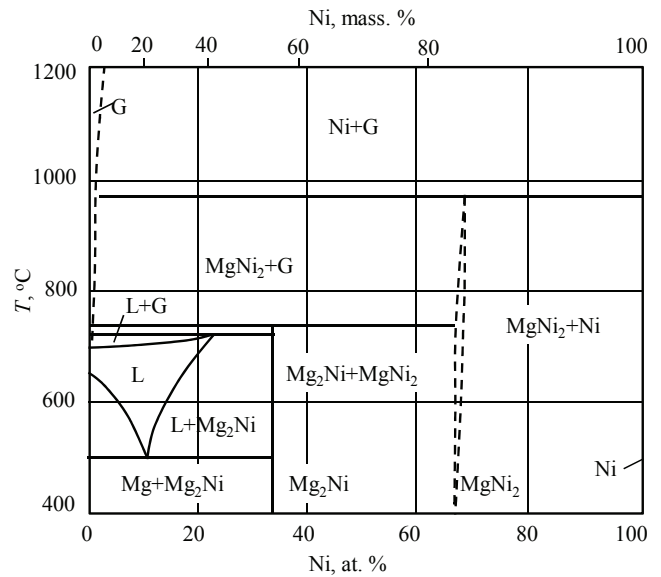


Fig. 3. Isobaric section of the state diagram of the Nickel-Magnesium system at a pressure of $p = 10^3$ Pa

Examples of such cross sections are shown in Figs. 3 and 4. The isobaric section of the state diagram of the nickel-magnesium system at a pressure $p = 10^3$ Pa is shown in Fig. 3. On the p - T diagram, the isobar $p = 10^3$ intersects four three-phase equilibrium curves: 5–11, 5–7, 3–7, and 4–8. In accordance with this, in the isobaric section of Fig. 3 there are four horizontal horizons of invariant equilibria. At 516 °C (intersection of the isobar with curve 5–11), the eutectic reaction $Mg \rightleftharpoons Mg_2Ni \rightleftharpoons L$ takes place. This part of the diagram is identical with the same part of the diagram in Fig. 1. At 720 °C (the intersection of the isobar with the curve 5–7 of the p - T diagram), the liquid decomposes with the release of Mg_2Ni and magnesium vapor.

At a temperature of 740 °C (the intersection of the isobar with the curve 3–7 of the p - T diagram) Mg_2Ni decomposes with the release of $MgNi_2$ and magnesium vapor. At 970 °C (the intersection of the isobar with the curve 4–8 of the p - T diagram) $MgNi_2$ decomposes into solid Ni and gas.

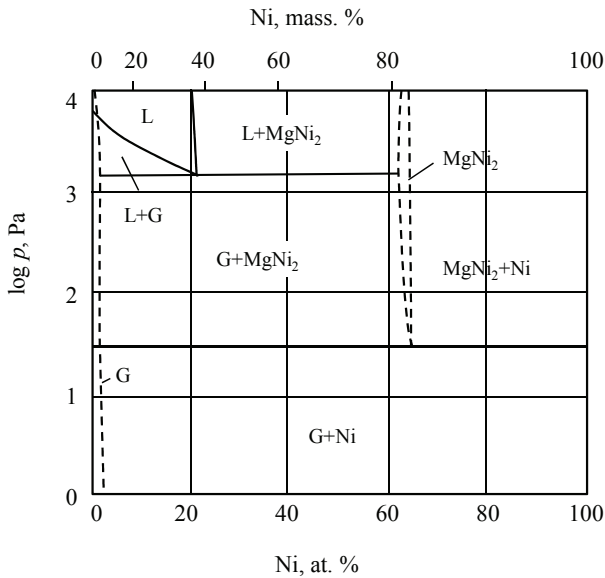


Fig. 4. Isothermal section of the state diagram of the nickel-magnesium system at a temperature of 800 °C

The isothermal section of the state diagram of the nickel-magnesium system at a temperature of 800 °C is shown in Fig. 4. The isotherm $T = 800\text{ °C}$ intersects in the p - T diagram two curves of three-phase equilibria 4-8 and 7-10. In accordance with this, on the isothermal section there are two horizontal horizons of non-invariant equilibria. At a pressure of 70 Pa (the intersection of the isotherm with curve 4-8 in the

p - T diagram), the MgNi_2 intermetallide decomposes into a gas consisting of magnesium vapor and solid nickel. At a pressure of $3 \cdot 10^3$ Pa (intersection of the isotherm with curve 7-10 in the p - T diagram), a liquid containing 200 at.% Ni decomposes into gas and the intermetallic compound MgNi_2 . The Mg_2Ni intermetallic compound is absent in the diagram in Fig. 4, since it decomposes incongruently into liquid and MgNi_2 at 760 °C.

The state diagram of Ni-Mg of the first kind [25] is presented in Fig. 5. This diagram represents single-phase fields below the curve 1-6-10, indicating the equilibrium vapor pressure over solid and liquid magnesium. The diagram of Fig. 5 is easily transformed from the p - T -diagram of Fig. 2 by eliminating from the last vertical lines the invariant equilibria with the participation of only condensed phases. The single-phase fields in Fig. 5 are separated by lines of two-phase equilibria. The solid sections of lines 5-7, 3-7, and 4-8 are plotted taking into account the experimental data [4, 6], the dashed sections are obtained by extrapolating these data. The phase compositions inside single-phase fields can be calculated using the data in Table 1.

Conclusion

Different variants of a graphic representation of the equilibrium in the nickel-magnesium system are proposed for variable values of pressure, temperature, and composition. The structure of the three-dimensional spatial image of the equilibrium is represented by the projection of the lines of maximum solubility on the temperature-composition plane, the projections of the lines of non-invariant equilibria on the pressure-temperature plane (p - T -state diagram), isobaric and isothermal section of the p - T -state diagrams, and the first-order state diagram in the p_{Mg} - T coordinates.

The presented versions of the equilibrium image can be useful in optimizing the technology for production and operation of nickel-magnesium alloys.

References

1. *Gidridnyye sistemy* [Hydride systems]. Handbook Ed. B.A. Kolacheva, A.A. Ilyina, V.A. Lavreiko, Yu.V. Levinsky. Moscow, Metallurgy, 1992, 352 p. (Rus)
2. Skryabina Nataliya, Artukov Valery, de Rango Patricia, Fruchart Daniel. Effect of temperature on firing process of Mg-Ni samples for fast formation of Mg_2Ni for hydrogen storage. *Int. J. hydrogen energy*, 2020, 45, 3008-3015.

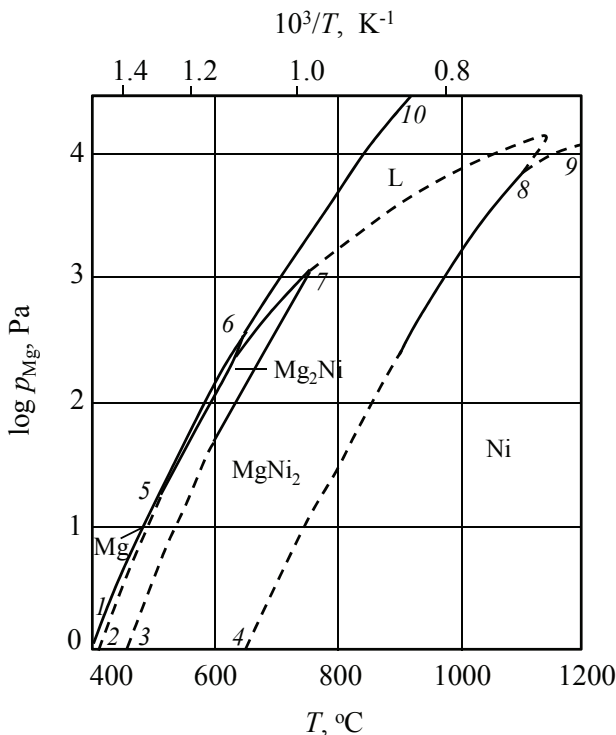


Fig. 5. The p_{Mg} - T -state diagram of the Ni-Mg system at $p_{\text{total}} \geq 10^4$ Pa

3. Jianling Huang, Hui Wang, Liuslhang Buyard, Jiangwen Liu, Min Zhu. Reducing the electrochemical capacity decay of milled Mg–Ni alloys: The role of stabilizing amorphous phase by Ti-substitution. *J. Power Sources*, 2019, 438 (226484), 1-8.
4. Yamada Y., Tajima K., Okada M., Tazawa M., Roos A., Yoshimura K. Dehydrogenation process of Mg–Ni based switchable mirrors analyzed by in situ spectroscopic ellipsometry. *Solar Energy Materials and Solar Cells*, 2012, 99, 84-87.
5. Wan Di-Qing, Wang Jin-Cheng, Wang Gai-Fang, Lin Feng, Zhi-Gang, Yang Gen-Cang. Effect of eutectic phase on damping and mechanical properties of as-cast Mg–Ni hypoeutectic alloys. *Trans. Nonferrous Met. Soc. China*. 2009, 19, 45-49.
6. Niaz N.A., Ahmad I., Waheed S., Khan S. Tajammul Hussain. Synthesis of Nanostructured Mg–Ni Alloy and Its Hydrogen Storage Properties. *J. Mater. Sci. Technol.*, 2012, 28 (5), 401-406.
7. Legan Hou, Bingcheng Li, Ruizhi Wu, Lin Cui, Peng Ji, Ruiying Long, Jinghua Zhanga, Xinlin Li, Anping Dong, Baode Sun. Microstructure and mechanical properties at elevated temperature of Mg–Al–Ni alloys prepared through powder metallurgy. *J. Mater. Sci. Technol.*, 2017, 33, 947-953.
8. Won Ha, Ho-Shin Lee, Jeong-Il Youn, Tae-Wan Hong, Young-Jig Kim. Hydrogenation and degradation of Mg–10 wt. % Ni alloy after cyclic hydriding-dehydriding. *Int. J. Hydrogen Energy*, 2017, 32 (12), 1885-1889.
9. Huaiyu Shao, Kohta Asano, Hirotohi Enoki, Etsuo Akiba. Preparation and hydrogen storage properties of nanostructured Mg–Ni BCC alloys. *J. Alloys and Comp.*, 2009, 477, 301-306.
10. Wei-hong Liu. The electrolyte temperature dependence of the electrochemical hydrogen storage property of Mg–Ni alloy codeposited from aqueous solution. *J. Alloys and Comp.*, 2005, 404-406, 694-698.
11. Skripnyuk V., Buchman E., Rabkin E., Estrin Y., Popov M., Jorgensen S. The effect of equal channel angular pressing on hydrogen storage properties of a eutectic Mg–Ni alloy. *J. Alloys and Comp.*, 2007, 436, 99-106.
12. Cermak J., Kral L. Ageing of Mg–Ni–H hydrogen storage alloys. *Int. J. Hydrogen Energy*, 2012, 37, 14257-14264.
13. Bobrovnichii G.S., Osipov A.S., Sideris A.J. Preparation of Mg–Ni alloys through high pressure treatment. *J. Alloy. and Comp.*, 2004, 372, 88-91.
14. Vijay R., Sundaresan R., Maiya M.P., Srinivasa Murthy S. Comparative evaluation of Mg–Ni hydrogen absorbing materials prepared by mechanical alloying. *Int. J. Hydrogen Energy*, 2005, 30, 501-508.
15. Čermák J., Král L. Hydrogen diffusion in Mg–H and Mg–Ni–H alloys. *Acta Materialia*, 2008, 56, 2677-2686.
16. Nogita K., Ockert S., Pierce J., Greaves M.C., Gourlay C.M., Dahlea A.K. Engineering the Mg–Mg₂Ni eutectic transformation to produce improved hydrogen storage alloys. *Int. J. Hydrogen Energy*, 2009, 34, 7686-7691.
17. Emmanuel Wirth, Darius Milcius, Constantina Filiou, Dag Noréus. Exploring the hydrogen sorption capacity of Mg–Ni powders produced by the vapour deposition technique. *Int. J. Hydrogen Energy*, 2008, 33, 3122-3127.
18. Samsonov G.V., Perminov V.P. *Magniytermiya* [Magnesium thermia]. Moscow: Metallurgiya, 1974, 176 p. (Rus)
19. Nayeb-Hashemi A.A., Clark J.B. The Mg–Ni (Magnesium–Nickel) System. *Bull. Alloy Phase Diagrams*, 1985, 6(3), 238-244.
20. *Diagrammy sostoyaniya dvoynnykh metallicheskih system* [State diagrams of binary metal systems]. Directory / Ed. N.P. Lyakisheva. V. 3, book 1. Moscow, Mashinostroyeniye, 1999, 872 p. (Rus)
21. Smith J.F., Christian J.L. Thermodynamics Formation of Copper-Magnesium and Nickel–Magnesium Compounds from Vapor Pressure Measurements. *Acta Metall.*, 1960, 8, 249-255.
22. Sieben P., Schmahl G. Vapor Pressure and Activity of Magnesium in Mg–Ni and Mg–Cu Binary Alloys. *Giesserei*, 1996, 18 (14), 197-211.
23. Tsai To Ngor, Serebryakov V.F. Davleniye para Mg nad Mg–Ni splavami [Mg vapor pressure over Mg–Ni alloys], *Izv. VUZov. Tsvetnaya metallurgiya*, 1984, 2b, 120-121. (Rus)
24. Tonkov E.Yu. *Fazovyye prevrashcheniya soyedineniy pri vysokom davlenii* [Phase transformations of compounds at high pressure]. Moscow, Metallurgy, 1988, 646 p. (Rus)
25. Levinsky Yu.V., Lebedev M.P. *p–T–x-diagrammy sostoyaniya dvoynnykh metallicheskih system* [The p–T–x-diagram of the state of binary metal systems]. Moscow: Nauchnyy mir, 2014, 200 p. (Rus)